

Monte Carlo study of diffraction in proton-proton collisions at $\sqrt{s} = 13$ TeV with the very forward detector

Qi-Dong Zhou^{*1} Yoshitaka ITOW^{1,2}, Takashi SAKO^{1,2}, and Hiroaki MENJO³

¹ *Institute for Space-Earth Environmental Research, Nagoya University, Nagoya, Japan*

² *Kobayashi-Maskawa Institute, Nagoya University, Nagoya, Japan*

³ *Graduate School of Science, Nagoya University, Nagoya, Japan*

E-mail: zhouqidong@isee.nagoya-u.ac.jp

Diffraction and non-diffractive collisions are totally different hadronic interaction processes, the diffractive processes are hardly predicted theoretically. This leads to the significant differences in the treatments of diffraction in the hadronic interaction models. Very forward detectors at colliders have unique sensitivity to diffractive processes, and they can be a powerful tool for studying diffractive dissociation by combining them with central detectors. Central information enables classification of the forward productions into diffraction and nondiffraction categories; in particular, most of the surviving events from the selection of diffraction belong to low-mass diffraction events which have not been measured precisely.

*The 3rd International Symposium on a Quest for the Origin of Particles and the Universe"
5-7 January 2017
Nagoya University, Japan*

*Speaker.

1. Introduction

The inelastic hadronic collisions are usually classified into *soft processes* and *hard processes*, according to the characteristics of the energy scales of hadron size and the momentum transfer. Most parts of the hard processes can be treated within the theoretical framework, based on the perturbative quantum chromodynamics (QCD) owing to the large momentum transfer. However, it is inadequate to describe the soft processes such as diffractive dissociations. Instead, a phenomenology of soft hadronic processes was employed to describe these processes at high energies, based on the Gribov-Regge theory [1, 2]. Therefore, it is extremely important to constrain the phenomenological parameters based on the measurement data for correct understanding of various diffractive processes and their accurate contribution to the total inelastic collisions.

In the present work, three subjects were investigated based on MC simulation. We first investigated the different contributions of nondiffractive and diffractive components to the forward neutral particle cross sections and the differences among models. Then, we evaluated the performance to identify the diffractive dissociation on the corresponding cross sections of neutral particles expected by the VF detector by applying a simple selection based on central detector information. Finally, we studied the sensitivity range in diffractive mass of the common experiment using VF and central detectors.

2. Diffractive dissociation

In high energy proton-proton interactions, the Regge theory describes diffractive processes as the t -channel reactions, which is dominated by the exchange of an enigmatic object with vacuum quantum numbers so called *Pomeron* [3]. There is an operational characteristic of diffractive interactions, which is a large angle separation between the final state systems so called rapidity gap $\Delta\eta$. The $\Delta\eta$ size and the location of them in the pseudorapidity phase-space can be used to determine the type of the diffractions, the relationship between the observable $\Delta\eta$ size and ξ_X is $\Delta\eta \simeq -\ln(\xi_X)$. where ξ_X is function of diffractive mass and M_X and center of momentum energy of \sqrt{s} , $\xi_X = M_X^2/s$. It is known that the $\Delta\eta$ size and inelasticity has relationship as $K_{inel} \simeq \exp(-\Delta\eta)$.

3. Diffractive and non-diffractive contributions to the LHCf photon spectra

As shown in Fig. 1, When ATLAS [4] and LHCf [5] observe the same collision, LHCf covers the very forward region and ATLAS has sensitivities to the central region. In this analysis, the



Figure 1: The LHCf detectors and their location.

event samples are classified into non-diffractive and diffractive collisions by using MC flags. The simulated photon spectra are shown in the right pads of Fig. 2 for a fiducial area of the LHCf analyses, $|\eta| > 10.94$. Clearly, the non-diffraction and diffraction implemented in each model are very different, especially, the diffractive contribution of PYTHIA8212DL has a big excess at the large energies. This leads to the big discrepancy between PYTHIA8212 and data, which are shown in the left pad of Fig. 2.

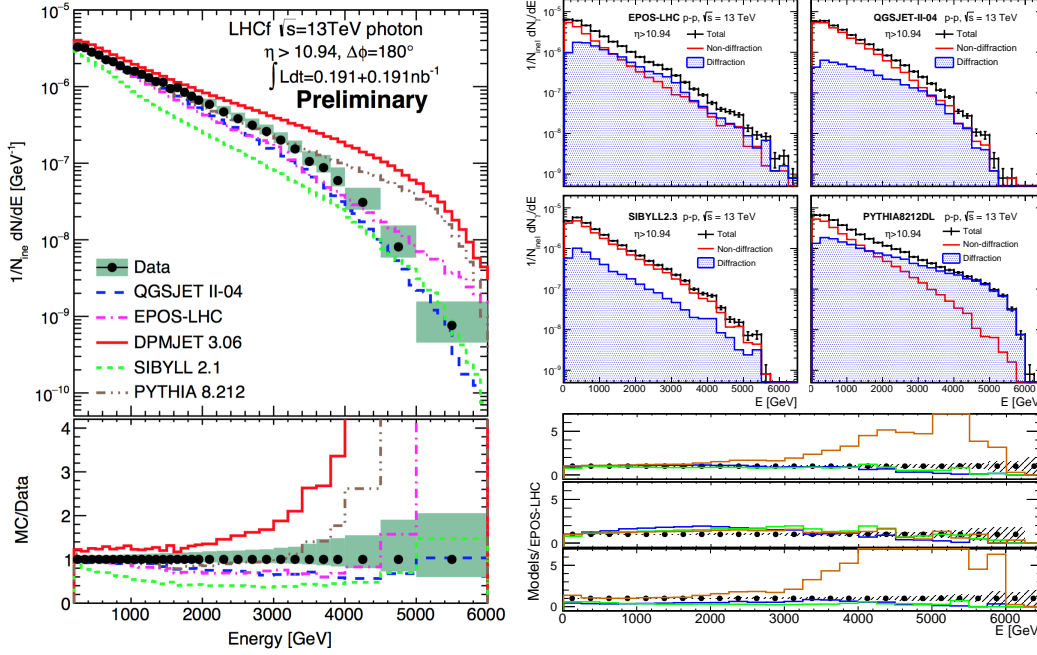


Figure 2: The LHCf photon spectra in pp collisions at $\sqrt{s} = 13$ TeV. The photon spectrum at $\eta > 10.94$ are shown by comparing with hadronic interaction models. The diffractive contribution of EPOS-LHC, QGSJET-II-04, SYBILL 2.3 and PYTHIA 8212DL are shown.

4. Identification of diffraction with ATLAS track information

4.1 Criteria of diffraction selection

Table 1: The efficiency and purity of diffraction selection with different ATLAS veto selection conditions.

Treatments	$N_{track}=0$	$N_{track} \leq 1$	$N_{track} \leq 2$	$N_{track} \leq 5$
Efficiency(ϵ)	0.493	0.556	0.619	0.691
Purity(p)	0.995	0.991	0.982	0.950

The identification of diffraction requires large rapidity gap, consequently small number of particles is expected in the central detector, for instance, the ATLAS detector. Basic idea in this analysis is if an event has a small N_{track} (the number of charged particles with $P_T > 100$ MeV at $|\eta| < 2.5$), it is more likely a diffractive event. In the other words, existence of charged tracks in the ATLAS rapidity range is used to veto non-diffractive events. It is assumed that the ATLAS

detector can count the number of charged particle tracks, N_{track} . Performance of ATLAS-veto event selection were studied for different criteria as listed in Table 1. According to MC true flags, events can be classified as non-diffraction (ND), central diffraction (CD), single diffraction (SD) and double diffraction (DD). By applying the ATLAS-veto selection to each event, the selection efficiency (ε) and purity (p) of diffractive event selection are defined as

$$\varepsilon = \frac{(N_{CD} + N_{SD} + N_{DD})_{ATLAS\ veto}}{N_{CD} + N_{SD} + N_{DD}} \quad (4.1)$$

$$p = \frac{(N_{CD} + N_{SD} + N_{DD})_{ATLAS\ veto}}{(N_{ND} + N_{CD} + N_{SD} + N_{DD})_{ATLAS\ veto}}. \quad (4.2)$$

where $N_{ND,CD,SD,DD}$ means number of event in each event category. The suffix $_{ATLAS\ veto}$ means number of event after applying the ATLAS-veto event selection. Consequently,

- no charged particle ($N_{track}=0$) in the kinematic range $|\eta| < 2.5$ and $p_T > 100$ MeV,

is adopted as ATLAS-veto selection condition.

4.2 The performance of ATLAS-veto selection

To evaluate the performance of the ATLAS-veto selection, the LHCf spectra were classified to non-diffractive-like and diffractive-like according to ATLAS-veto selection. The accurate performances of the selection were evaluated by adapting the Eq.4.1 and Eq.4.2 to the LHCf photon spectrum. As shown in Figs.3, it is clear that selection purity stays constantly high (at $\approx 100\%$), independent of particle type, energy, and MC simulation model, whereas selection efficiency has a tendency to increase with increasing energy. In contrast to selection purity, selection efficiency exhibits differences among MC simulation models. The more detail information was shown in [6].

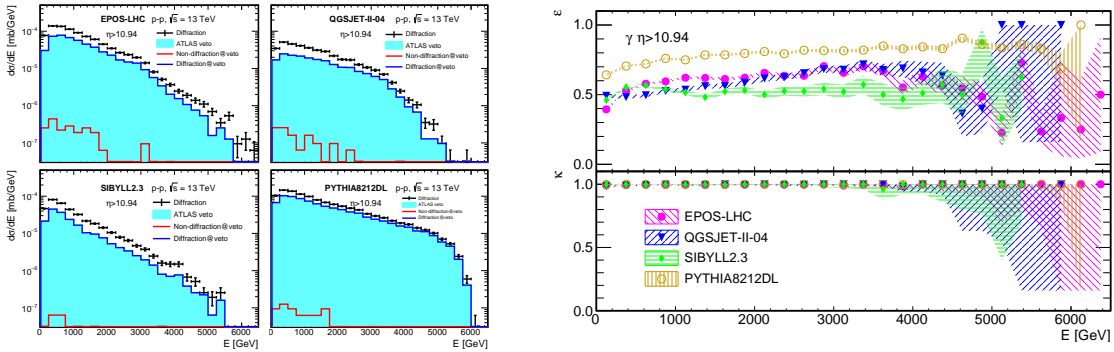


Figure 3: The left figure shows photon spectra at $\eta > 10.94$ generated by EPOS-LHC, QGSJET-I I-04, SYBILL 2.3, and PYTHIA 8212DL. The top four panels show the spectra of true diffraction (black points) and diffractive-like events corresponding to ATLAS-veto selection (filled gray areas), in addition, the ATLAS-veto events were classified by nondiffraction (red) and diffraction (blue) again according to MC true information. The right figure shows the efficiency and purity of diffraction selection by using ATLAS-veto technique correspond to up and down pads on the figure of right side.

4.3 Low-mass diffraction

According to QGSJET-II-04 simulation predictions, most of the LHCf detected events survived from the ATLAS-veto selection are from the low-mass diffraction as shown in Fig.4. In particular, all the LHCf detected low-mass diffractive events at $\log_{10}(\xi_x) < -5.5$ survived from the ATLAS-veto selection. Therefore, the forward detector combine with central detector can give a constraint to the treatment of low-mass diffraction implemented in the MC simulation models.

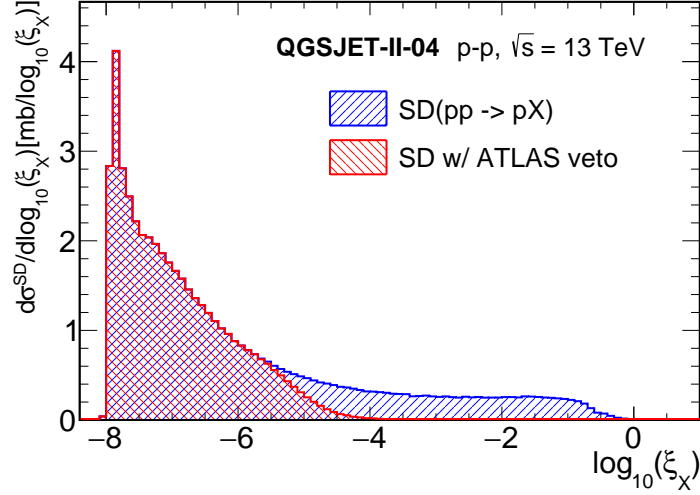


Figure 4: The SD ($pp \rightarrow pX$; blue) cross section as a function of $\log_{10}\xi_x$ predicted by using QGSJET-II-04 MC samples. Which is compared with the SD cross section after applying the ATLAS-veto selection (red).

5. Conclusions

Non-diffraction and diffraction have different contribution in the very forward regions, the predictions of hadronic interaction models also exhibit big discrepancies among each other. The rapidity gap measurement (central-veto technique) using central information is an effective way to identify diffractive events and classify the forward productions to nondiffraction and diffraction. Furthermore, using the observed events, it is capable of both constraining the differential cross sections ($d\sigma/dE$, $d\sigma/d\eta$) of low-mass diffraction and helping to identify the inherent problems in the models corresponding to low-mass diffraction.

References

- [1] V. Gribov, Sov. Phys. JETP **30**, 414 (1968).
- [2] T. Regge, Nuovo, Ciment **14**, 951–976 (1959).
- [3] E. Feinberg, I. Pomerancuk, Suppl. Nuovo Cim. **3**, 652 (1956).
- [4] ATLAS Collaboration, JINST, **3**, S08003 (2008)
- [5] LHCf Collaboration, JINST, **3**, S08006 (2008)
- [6] Qi-Dong Zhou et al., arXiv: 1611.07483. Accepted by Eur. Phys. J. C.